Analytical and Bioanalytical Chemistry (2021) 413:6813–6821
https://doi.org/10.1007/s00216-021-03637-5

RESEARCH PAPER

A novel nickel-modified nano-magnetite for isolation of histidine-tagged proteins expressed in *Escherichia coli*

Liang Ma[1] · Yindi Zhu[1] · Xueming Chen[1] · Raohao Fang[1] · Yuru Chen[1] · Xia Xu[1,2] · Guozheng Huang[1] · Zi Liu[1] · Xiang Liu[1]

Received: 14 May 2021 / Revised: 20 July 2021 / Accepted: 27 August 2021 / Published online: 7 September 2021

Abstract

Nano-magnetite with superparamagnetism could be coated by some organic compounds or by nano Au or Pt via surface modifications with multi-step reactions for the applications of isolating histidine-tagged (His-tagged) proteins. Introducing active sites of binding histidine onto the surface of nano-magnetite was the ultimate task. However, multi-step treatments might result in departure of the coatings from the surface of the nano-magnetite, which led to loss of active sites. In this work, we reported a convenient and efficient way of treating nano-magnetites and applied them in isolating His-tagged proteins. Carboxylates were introduced on the surface of home-made nano-magnetite directly via ultrasonic mixing with sodium bitartrate rather than complicated surface modifications, which was proved by thermogravimetric analyses. Ni^{2+} was, therefore, caught by the carboxylates of the coating via the coordinate interaction, demonstrated by X-ray photoelectron spectra. The coated magnetic nanoparticles with the bonded Ni^{2+} were successfully employed to selectively bind and separate recombinant His-tagged proteins directly from the mixture of *Escherichia coli* cell lysate, and showed wonderful affinity for His-tagged proteins with the saturated adsorption amount being 556 mg g^{-1}. Additionally, such functionalized nano-magnetite manifested the excellent recyclability in isolating His-tagged proteins.

Keywords Nano-magnetite · Sodium bitartrate · Nickel cation · Histidine-tagged protein purification

Introduction

The use of DNA recombinant technology to express tagged fusion proteins is among the most favorable strategies for large-scale production and purification of proteins. Histidine tag (His-tag) is widely used to expedite the separation of recombinant proteins from a crude lysate. Magnetites with nanoscale were applied extensively in the biological domain depending on its superparamagnetism according to recent reports. Due to the cheap raw materials, easy preparation, and efficient coating for constructing a target interface, nano-magnetite provided an economical approach of isolating and purifying proteins. Various techniques were invented to build a favorable interface for docking Ni^{2+} [1–3], Cu^{2+} [4], or Co^{2+} [5], which provided active sites for the coordination with His-tagged proteins. N_{α},N_{α}-bis(carboxymethyl)-L-lysine hydrate (or aminobutyl nitrilotriacetic acid, abbreviated as ANTA) was applied commonly in catching Ni^{2+} due to the chelation between the carboxyl groups and Ni^{2+} [2, 6]. Several approaches were explored for binding ANTA onto the surface of nano-magnetites via a reaction between primary amino of ANTA and surface functional groups of magnetite [3, 5, 7–9]. For example, ANTA could be involved in the combination with surface epoxy groups of nano-magnetite via the addition reaction between the primary amino of ANTA and the epoxy [8, 9]. During the process, the first step of coating magnetite with a proper chemical reagent was vital. On the one hand, the affinity between the reagent and magnetite should be firm and stable. On the other hand, such coating should possess proper terminal groups with chemical reactivity that could be involved in the successive chemical modifications or the

✉ Zi Liu
liuz2014@ahut.edu.cn

✉ Xiang Liu
liuxiang@ahut.edu.cn

[1] Department of Chemical Biology and Pharmaceutical Engineering, School of Chemistry and Chemical Engineering, Anhui University of Technology, Ma'anshan 243002, Anhui, China

[2] Biochemical Engineering Research Center, Anhui University of Technology, Ma'anshan 243002, Anhui, China

coordination with Ni^{2+} directly. Generally, it was accepted that there were hydroxyls on the surface of nano-magnetites [8, 10]. Thus, silane coupling agents with various end functional groups could be linked with nano-magnetite [1, 3, 8, 10–13]. For instance, nano-magnetite could be coated directly by 3-(trimethoxysilyl)propyl methacrylate [12]. The terminal C=C involved further reaction of copolymerization with glycidyl methacrylate. Successively, iminodiacetic acid reacted with the end epoxy group for introducing the carboxyl groups on the surface of nano-magnetites. 4-Vinylbenzyl chloride could also take part in the copolymerization with the end C=C. The terminal chlorine could be substituted by imino of iminodiacetic acid [10]. The introduced carboxyl groups played a key role of catching Ni^{2+}. Iminodiacetic acid could also be combined with 3-glycidoxypropyltrimethoxysilane firstly. Then, carboxylates were introduced directly onto the surface of nano-magnetite via the interaction between nano-magnetite and trimethoxysilane [13]. These approaches of introducing carboxyl groups on the surface of nano-magnetites were more inexpensive than that of introducing ANTA. Replacement of ANTA with iminodiacetic acid and application of a silane coupling agent realized the activation of nano-magnetite and reduced the experimental costs obviously. However, the silane coupling agent was apt to hydrolyze in aqueous medium that declined the effectiveness of coating. In fact, coating nano-magnetite depended mainly on the treatment of the first step. The weak interaction between the polarized surface of magnetite and coating could not endure intensive disturbing during successive chemical modifications for introducing carboxyl groups. It was possible that the introduced iminodiacetic acid or ANTA was inclined to leave from the surface of nano-magnetite finally. Therefore, more attentions should be paid on coating in the first step for realizing the intensive interaction between the coating and magnetite.

Several reports about coating Au or Pt on the surface of nano-magnetites had been published recently [14–16]. The intensive interaction between surface Au or Pt and 3-mercaptopropionic acid favored the introducing of ANTA during the next steps for realizing binding of Ni^{2+} or Co^{2+} via the coordination. However, such a way of coating with Au or Pt was troublesome and costly. Comparatively, coating nano-magnetite directly with organic compounds which play a role of immobilizing Ni^{2+} was more efficient and convenient. For example, nano-magnetite could be coated directly by histidine which depended on the intensive interaction between carboxyl of histidine and surface hydroxyl of magnetite [17]. The terminal imidazole undertook the affinity with Ni^{2+}, which performed well in purifying His-tagged proteins.

Herein, we provided a convenient approach of direct coating nano-magnetite with sodium bitartrate for immobilizing Ni^{2+} and realizing efficient isolation of His-tagged proteins. The sodium bitartrate with several polar functional groups played the dual roles of coating magnetite and catching Ni^{2+}. Compared with conventional immobilized metal affinity chromatography (IMAC)–based affinity methods and protocols based on affinity magnetic nanomaterials, the NM-SB-Ni used in this article avoided time-consuming operation for protein separation and complicated chemical modifications step by step for nanoparticle preparation. The inexpensive raw materials and gentle conditions of preparing the nano-magnetite as well as the facile approach of docking Ni^{2+} reduce the cost of protein isolation.

Materials and methods

Chemical reagents

Ferric chloride hexahydrate (99%), ferrous chloride tetrahydrate (99%), sodium hydroxide (97%), and sodium bitartrate monohydrate (≥ 99.0%) were purchased from Aladdin Company (Shanghai, China) and used without further purification. A protein molecular weight marker (catalog no. 26616) was purchased from Thermo Fisher Scientific (Waltham, MA, USA). Double distilled water was used throughout the whole work.

Preparation of nano-magnetite and the coating with sodium bitartrate

Solutions of ferric chloride and ferrous chloride were mixed at 25 °C according to the molar ratio of 1:2. The mixture was agitated violently and was alkalized with dropwise NaOH solution (0.5 mol L^{-1}) until the pH reached 11.0. The agitation lasted for more than 24 h. The color of the reactants changed from dark green to brown gradually during the reaction. The complete brown indicated finish of the reaction. The purification of the nano-magnetite was realized conveniently with a magnetic rod. The nano-magnetite particles were collected (represented with NM) and stored in aqueous media.

Such a mixture of 30 mL (containing 45.5 mg nano-magnetite) was mixed with 0.45 g sodium bitartrate in a beaker and disposed ultrasonically for 4 h at room temperature. A magnetic rod was placed outside the beaker for collecting magnetic solids and the aqueous solution in the mixture was dumped. The magnetic solids were washed with 50 mL water and collected with a magnetic rod. Such a process was repeated for four times for removing any free sodium bitartrate. Finally, nano-magnetite coated by sodium bitartrate was obtained (represented with NM-SB), which was stored in an aqueous medium.

Immobilization of Ni^{2+} with NM-SB

A 20-mL NM-SB suspension was measured and mixed with 50 mL $NiSO_4$ solution (0.17 mol L^{-1}). The mixture was

treated ultrasonically for 4 h for realizing binding of Ni^{2+}. The excess Ni^{2+} was removed. Then, 50 mL water was added in with stirring for removing the free Ni^{2+}. The magnetic particles were collected and washing was repeated. These processes were cycled for three times for removing any free Ni^{2+}. The products were represented with NM-SB-Ni.

Characterization techniques

The pattern of prepared nano-magnetite was characterized by X-ray powder diffraction (D8 ADVANCE, BRUKER Company). The morphology was checked by image of transmission electron microscopy (TEM, Tecnai G2 F20 S-TWIN, FEI Company). Thermogravimetric estimation (Thermax 700, Thermo Fisher Scientific) with flowing nitrogen gas and a heating rate of 10 °C min^{-1} demonstrated the surface coatings of nano-magnetites. The immobilization of Ni^{2+} was demonstrated by X-ray photoelectron spectrum (KRATOS AMICUS). Wide scan over a binding energy of 0–1350 eV and high-resolution scans (step = 0.05 eV) were executed for obtaining the surface ingredient and elemental information. C 1s spectrum was deconvoluted in nonlinear least-square fitted for obtaining the C 1s signal in different environments.

Preparation of His-tagged proteins

In this study, two different His-tagged proteins were prepared. His-tagged human carbonic anhydrase II (his-hCA II) protein was expressed and purified via procedures reported in our previous study [18]. His-hCA II containing a hexahistidine sequence tagged at the C-terminus was designed, synthesized, and cloned into pET-30a (+) plasmid using *Nde* I and *Hind* III restriction sites by GeneScript (GeneScript, USA), and human peptidyl-prolyl *cis/trans* isomerase NIMA-interacting 1 (*PIN1*) gene with hexahistidine sequence tagged at the C-terminus (his-Pin1) was designed, synthesized, and cloned into pET-28a (+) plasmid using *Nco* I and *Xho* I restriction sites by Synbio Tech (Synbio Technologies, Suzhou, China). His-Pin1 recombinant plasmids were transformed into *Escherichia coli* (*E. coli*) BL21 (DE3) (Novagen, Merck, Shanghai, China) using standard protocols. The transformed cells were grown to OD600 of 0.6 in Luria-Bertani (LB) medium containing 100 μg/mL of kanamycin at 37 °C and 220 rpm, induced with 0.2 mM isopropyl β-D-thiogalactopyranoside (IPTG) for 6 h, and pelleted at 4000 rpm. The cells were resuspended in lysis buffer (50 mM Tris, 150 mM NaCl, 5% glycerol pH 8.0) and disrupted using a sonicator (Xinzhi Biotech, Ningbo, China) in an ice bath for 20 min at 200 W. After centrifuged at 15,000 rpm for 10 min, the supernatant and cell debris were collected, and SDS-PAGE and Coomassie brilliant blue R-250 staining assay were conducted to detect the expression level of his-Pin1. Protein concentration was determined using a Bradford assay. The supernatants of *E. coli* cell lysate containing his-hCA II or his-Pin1 proteins were used for enrichment and separation experiments.

Enrichment and separation of His-tagged proteins from *E. coli* cell lysate using NM-SB-Ni

NM-SB-Ni (200 μL, 1.87 mg mL^{-1}) nanoparticles were separated from the solution using DynaMag™ Spin Magnet (Life Technology). Then, 300-μL diluted supernatant of *E. coli* cell lysate containing his-hCA II or his-Pin1 was added directly into nanoparticles and rotated for 1 h at 4 °C. The nanoparticles having captured His-tagged proteins were isolated from the solution using magnet and washed with 300 μL washing buffer (50 mM Tris, 150 mM NaCl, 50 mM imidazole at pH 7.5) to reduce the non-specific interactions. After that, the trapped His-tagged proteins were eluted from targeting nanoparticles by the addition of an elution buffer (50 mM Tris, 150 mM NaCl, 250 mM imidazole at pH 7.5) with a volume of 300 μL and rotated at 4 °C for 10 min. The protein solutions collected at each step were detected by SDS-PAGE and Coomassie brilliant blue R-250 staining assay. Equal amounts of NM and NM-SB were used for isolating his-hCA II from cell lysate using the above method. To confirm the binding specificity of the nanoparticles for the separation and purification of His-tagged proteins, 300-μL supernatant of *E. coli* cell lysate containing his-hCA II was incubated with different concentrations of NM-SB-Ni (0.3, 0.6, 0.9, 1.2, 1.5 mg mL^{-1}), and enrichment and separation were conducted using the same method as above.

Detection of binding capacity of NM-SB-Ni

In this work, purified his-hCA II proteins were employed as a protein model for investigation of the adsorption capacity of NM, NM-SB, and NM-SB-Ni. Briefly, nanoparticles (50 μg) were mixed with purified his-hCA II proteins in lysis buffer (50 mM Tris, 150 mM NaCl, 5% glycerol pH 8.0) at different concentrations in a centrifuge tube and rotated for 1 h at 4 °C. Afterwards, the supernatants were collected separately by an external magnet and the content of protein was detected by the Bradford method with bovine serum albumin as a standard. The adsorption amount (Q_e, mg g^{-1}) of nanoparticles was calculated based on the following formula:

$$Q_e = \frac{(C_0 - C_s)}{m} V \quad (1)$$

where C_0 (mg mL^{-1}) is the initial protein concentration, C_s (mg mL^{-1}) is the protein concentration in supernatant at adsorption equilibrium, V (mL) is the volume of protein solution, and m (g) is the mass of nanoparticles.

The adsorption isotherms were fitted by the Langmuir model:

$$Q_e = \frac{Q_m C_s}{K_d + C_s} \quad (2)$$

where Q_m (mg g^{-1}) is the saturated adsorption amount and K_d is the decomposition rate [19].

Reusability of NM-SB-Ni

Briefly, 200 μL of NM-SB-Ni nanoparticles was separated from the solution using DynaMag™ Spin Magnet (Life Technology), and then 300 μL of diluted his-hCA II cell lysates was added and incubated for 1 h at 4 °C. Then, magnetic separation was conducted and the captured his-hCA II proteins were washed with washing buffer (50 mM Tris, 150 mM NaCl, 50 mM imidazole at pH 7.5) and eluted with 300 μL elution buffer (50 mM Tris, 150 mM NaCl, 250 mM imidazole at pH 7.5). After washed several times, the recovered nanoparticles were reused for protein separation experiment. The total experimental process was repeated for 6 times, and the eluate containing his-hCA II proteins in each time was collected and used for SDS-PAGE analyses.

Results and discussion

Preparation of nano-magnetite and coating by sodium bitartrate

The procedure for the preparation of NM-SB-Ni nanoparticles was schematically illustrated in Scheme 1. The synthesized nano-magnetites were proved by measurement of X-ray powder diffraction, which is revealed in the inset of Fig. 1(a). The diffraction peaks at 18.43, 30.08, 35.49, 37.05, 43.07, 53.58, 57.01, 62.65, and 74.32° correspond to crystal planes of (111), (220), (311), (222), (400), (422), (511), (440), and (622), respectively, which matches well with the standard JCPDS no 19-0629 (inset of Fig. 1(a)) and is consistent with reported literatures [3, 16, 20]. The fact demonstrates that nano-magnetite is apt to be synthesized under very mild conditions rather than violent disposing [1, 10, 21].

The image of transmission electron microscopy exhibited the morphology of the as-prepared nano-magnetite, which is shown in Fig. 1(a). The bare nano-magnetite was apt to accumulate because of the large specific areas and precipitate in aqueous medium. The particle sizes were less than 25 nm and size distribution was unhomogeneous, which is exhibited in Fig. 1(b). According to our experiments, sodium bitartrate can be a well candidate for stabling nano-magnetite in an aqueous medium depending on the hydroxyl, carboxyl, and carboxylate groups. Figure 1(c) reveals that the surface of the nanoparticles was coated by something like membranes marked by several dashed circles. The interactions between polar functional groups of sodium bitartrate and nano-magnetites help enhance dispersing stability that favors for successive coordination with Ni^{2+}. Thermogravimetric curves of Fig. 1(d) proved that the velocity of weight loss of NM-SB was greater than that of the bare nano-magnetites, which was due to the decomposition of surface coating of nano-magnetites. This declares that the nano-magnetites are coated by sodium bitartrate. Additionally, weight loss of the nano-magnetites reaches 4% approximately when the temperature arrives at 800 °C. It suggests there are some polar functional groups on the surface of the nano-magnetites such as hydroxyls [8], which attached with the nano-magnetites covalently. This is favorable for the attachment with sodium bitartrate.

Nano-magnetites coated by sodium bitartrate were also proved by X-ray photoelectron energy spectra of NM-SB-Ni, which are indicated in Fig. 2. In Fig. 2(a), peak 284.8 eV forecasts the surface C-C species. Band 286.2 eV should be assigned to C–O ingredient. Binding energy of 288.7 eV is due to the surface carboxyl group of O=C–O– [22]. Such evidences confirm that sodium bitartrate is docked on the surface of nano-magnetite successfully. Sodium bitartrate plays the roles of not only coating nano-magnetites but also affinity for Ni^{2+} which proved by Fig. 2(b) of Ni 2p signals. Binding energies of 855.5 and 861.2 eV are assigned to Ni 2p3/2 and Ni 2p1/2 respectively [3]. The atomic percentages of elemental Ni, C, O, and Fe on the NM-SB-Ni surface are 1.97, 32.37, 46.41, and 19.25%, respectively. The lower ingredient of Fe forecasts the surface of nano-magnetites is covered by sodium bitartrate.

Application of NM-SB-Ni in isolating His-tagged proteins from real samples

In this work, we first employed crude cell lysate from *E. coli* containing recombinant expressed his-hCA II proteins to evaluate the applicability of NM-SB-Ni nanoparticles as an adsorbent for highly selective isolation of His-tagged proteins from real samples. Whole procedures of enrichment and separation are illustrated in Scheme 1.

Human CA II is a carbonic anhydrase that can catalyze CO_2 hydration into bicarbonate (HCO_3^-). This protein was successfully expressed at high levels with a His-tag at its C-terminus in *E. coli* in our previous work for the application of CO_2 capture [18]. From the results of SDS-PAGE analysis shown in Fig. 3(a), the band of expressed his-hCA II proteins (about 31 kD, marked with a horizontal arrow) was clearly observed along with other unrelated bacterial proteins in the crude cell lysate (lane 1). This band has obviously disappeared or weakened in the supernatant and become predominant in eluate after adsorption by NM-SB-Ni (Fig. 3(a), lanes 2–3),

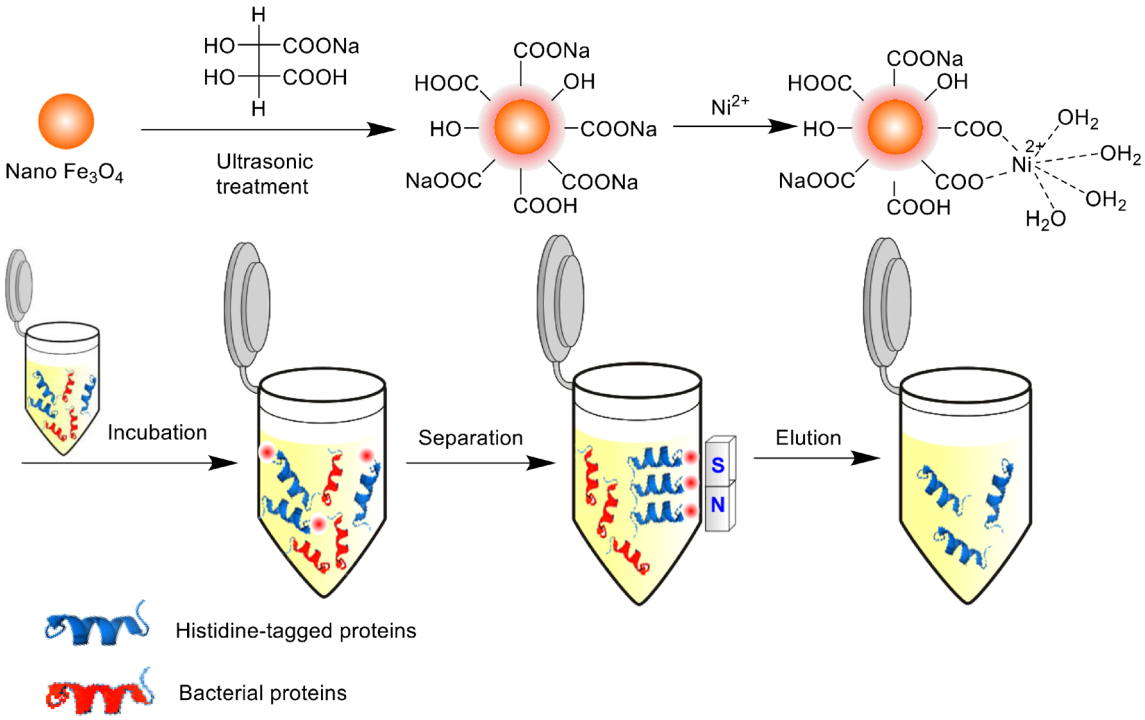

Scheme 1 Schematic representation of preparation of NM-SB-Ni nanoparticles and the procedure of enrichment and separation of His-tagged proteins from crude *E. coli* lysate

indicating that NM-SB-Ni could efficiently capture and separate his-hCA II proteins. In order to further verify the practical application of this method, another recombinant protein with his-tag (his-Pin1) was used. Human peptidyl-prolyl cis/trans isomerase NIMA-interacting 1 (PIN1), which specifically binds to phosphorylated ser/thr-pro motifs of a subset of phosphorylated proteins to regulate its conformation, has been shown to play a critical role during oncogenesis [23]. His-

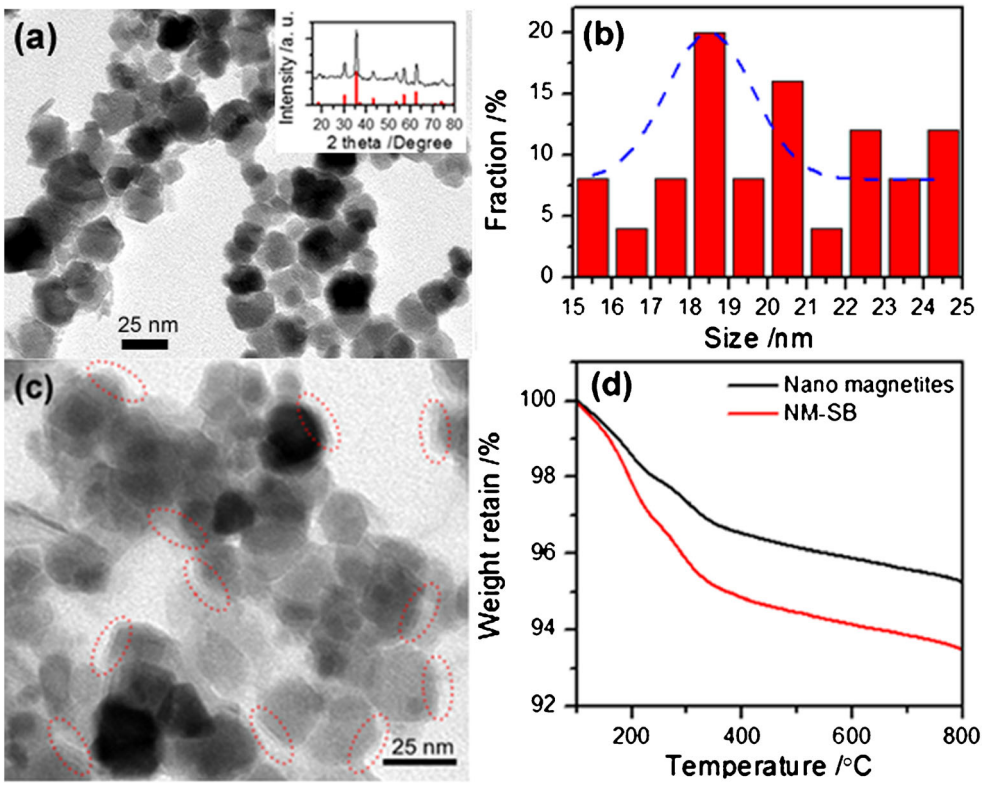

Fig. 1 Images of transmission electron microscopy (**a**) and size distribution (**b**) of as-prepared nano-magnetites. Images of transmission electron microscopy of NM-SB (**c**) and thermogravimetric curves of the nano-magnetites and NM-SB (**d**). X-ray powder diffraction pattern shown in the inset of (**a**) demonstrates the synthesized nano-magnetites

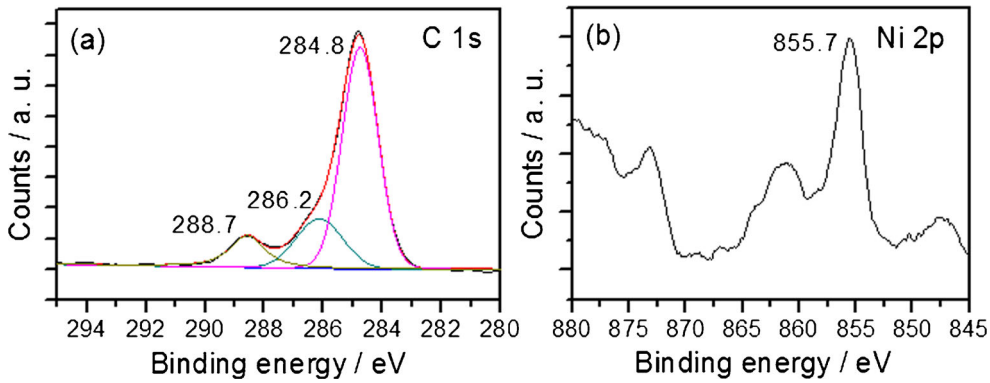

Fig. 2 X-ray photoelectron energy spectra of NM-SB-Ni with high-resolution on C (**a**) and Ni (**b**)

Pin1 prokaryotic expression vector had been constructed in our lab for investigating the function of this protein in cancer. By using *E. coli* cell lysate containing His-Pin1 proteins, we found that NM-SB-Ni nanoparticles could also efficiently capture and separate this protein (Fig. 3(b)). Besides, NM and NM-SB could not isolate his-hCA II proteins from the cell lysate, which is shown in Fig. 3(c), indicating the specific binding of NM-SB-Ni to His-tagged proteins.

To further explore the detailed binding specificity of the nanoparticles for His-tagged proteins, *E. coli* cell lysate containing his-hCA II proteins was incubated with NM-SB-Ni with different concentrations. As can be seen from Fig. 4(a), his-hCA II proteins in eluate gradually increase with the increase of nanoparticle concentration. More importantly, his-hCA II proteins in supernatant fractions gradually decrease with incremental concentration of NM-SB-Ni, while unrelated bacterial proteins in supernatant are not changed obviously (Fig. 4(b)), indicating the high specificity of this nanoparticle for the separation and purification of His-tagged proteins.

These results prove that NM-SB-Ni nanoparticles reported in this study are promising hosts for the efficient separation and purification of His-tagged proteins from complex cell lysate.

Detection of binding capacity of NM-SB-Ni

To explore the binding capacity of the nanoparticles for His-tagged proteins, purified his-hCA II proteins were used as a model protein. A certain amount of NM, NM-SB, and NM-SB-Ni nanoparticles was incubated with solutions containing purified his-hCA II proteins with different concentrations and the content of proteins bound on nanoparticles was tested. As shown in Fig. 5, adsorption capacities of NM-SB-Ni for His-tagged proteins increased with the increase of the initial protein concentration, and the saturated adsorption of his-hCA II proteins was gradually achieved with further increase of the concentrations, while the adsorption capacity of NM and NM-SB particles dramatically lowers than that of NM-SB-Ni, further proving the specific binding of NM-SB-Ni to His-tagged

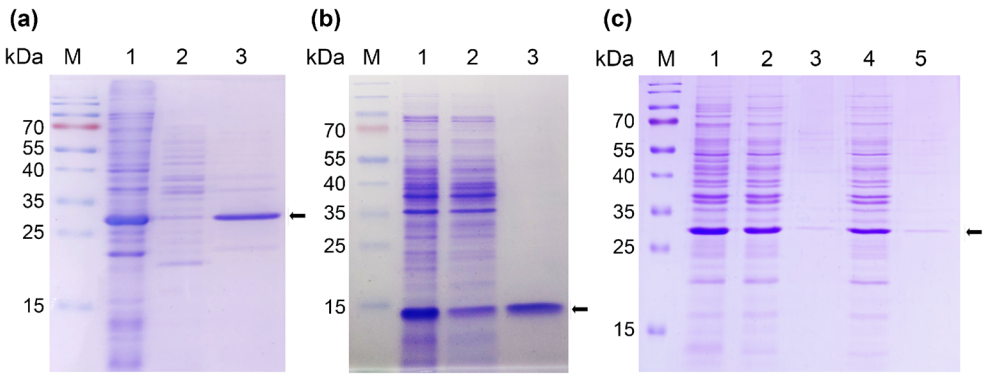

Fig. 3 (**a**) SDS-PAGE analysis of purification of overexpressed his-hCA II proteins from *E. coli* lysate using NM-SB-Ni nanoparticles. Lane M, molecular marker; lane 1, cell lysate containing his-hCA II proteins; lane 2, supernatant of cell lysate after adsorption; and lane 3, eluate from NM-SB-Ni after adsorption. (**b**) SDS-PAGE analysis of purification of overexpressed his-Pin1 proteins from *E. coli* lysate using NM-SB-Ni nanoparticles. Lane M, molecular marker; lane 1, cell lysate containing his-Pin1 proteins; lane 2, supernatant of cell lysate after adsorption with NM-SB-Ni nanoparticles; and lane 3, eluate from NM-SB-Ni after adsorption. (**c**) SDS-PAGE analysis of adsorption by NM and NM-SB nanoparticles from *E. coli* lysate containing his-hCA II proteins. Lane M, molecular marker; lane 1, cell lysate; lane 2, supernatant of cell lysate after adsorption by NM; lane 3, eluate from NM nanoparticles after adsorption; lane 4, supernatant of cell lysate after adsorption by NM-SB; and lane 5, eluate from NM-SB nanoparticles after adsorption

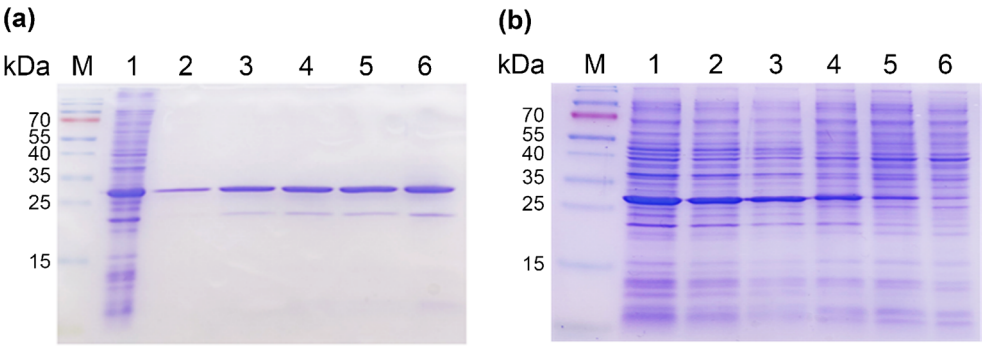

Fig. 4 *E. coli* cell lysate containing his-hCA II proteins was incubated with NM-SB-Ni with different concentrations. Lane M, molecular marker; lane 1, cell lysate containing his-hCA II proteins; lanes 2–6(a), his-hCA II proteins washed off from NM-SB-Ni nanoparticles with different concentrations; and lanes 2–6(b), supernatant of cell lysate after adsorption

Table 1 Binding capacity of some Ni-chelating adsorbents for purification of His-tagged recombinant proteins reported in the literatures

Materials	Binding capacity (mg g^{-1})	Reference
$CMPEI_2$-Ni^{2+}@SiO_2@Fe_3O_4	206	[24]
Fe_3O_4@Ni^{2+}-NTA-PS	163.52	[7]
$MnFe_2O_4$@SiO_2@Ni-Salen	180	[25]
Fe_3O_4@Histidine-Ni	700	[17]
Fe_3O_4@SiO_2@ poly(GMA-DEA)@poly(GMA-IDA)@Ni^{2+}	250	[26]
Fe_3O_4/Cys-Ni^{2+}	53.2	[27]
$MnFe_2O_4$@SiO_2@NH_2@2AB-Ni	220	[28]
NM-SB-Ni	556	This work

proteins. The Langmuir model was applied to analyze the adsorption data of his-hCA II proteins, and the saturated adsorption amount (Q_m) of NM-SB-Ni for his-hCA II proteins was found to be 556 mg g^{-1}, which was much higher than those of commercial microbeads (< 20 mg g^{-1}) [14]. Table 1 lists the binding capacity of other Ni-chelating adsorbents for purification of His-tagged proteins in reported references. It is clear that NM-SB-Ni nanoparticles provide a higher adsorption for His-tagged proteins with respect to other Ni-chelating materials. However, it should be noted that this comparison could not be very exact because the nature of recombinant proteins may also influence the adsorption parameter.

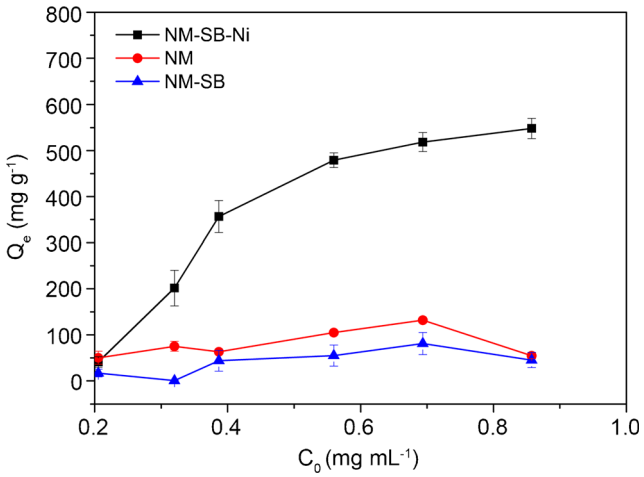

Fig. 5 Adsorption capacity of NM, NM-SB, and NM-SB-Ni nanoparticles

Recyclability of the magnetic nanoparticles for His-tagged protein separation

The recyclability is one of the most important properties for the application of adsorbents. Herein, the recyclability of NM-SB-Ni was investigated by performing the adsorption (isolation)-elution process using *E. coli* cell lysate containing recombinant expressed his-hCA II proteins. The recycling experiments were carried out for six successive cycles under the same experimental conditions. As shown in Fig. 6, the separation capability of NM-SB-Ni is more than 90% after six cycles of reuse, indicating the excellent stability and recyclability of this nanoparticle as an adsorbent.

Conclusions

In this study, we developed a facile and economical method for the preparation of NM-SB-Ni magnetic nanoparticles. NM-SB-Ni could specifically bind and separate His-tagged proteins from *E. coli* cell lysate with high efficiency, and its saturated adsorption amount for purified His-tagged proteins was estimated to be 556 mg g^{-1}. Moreover, NM-SB-Ni

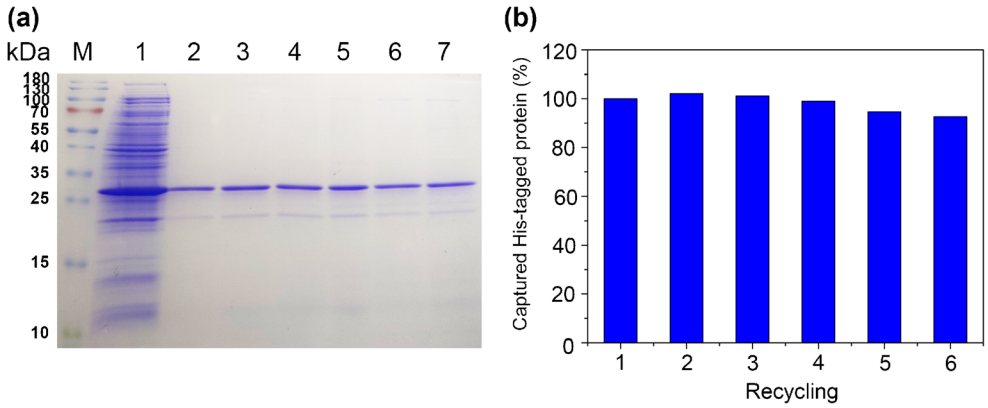

Fig. 6 The recycling capacity of the NM-SB-Ni nanoparticles for separation of his-hCA II proteins from *E. coli* lysate. (**a**) SDS-PAGE analysis. Lane M, molecular marker; lane 1, cell lysate containing his-hCA II proteins; and lanes 2–7, the his-hCA II proteins washed off from NM-SB-Ni nanoparticles reused up to six times. (**b**) The semi-quantitative result of isolated his-hCA II proteins after each cycle evaluated by normalizing the binding amount at each cycle in ratio to the first cycle on the SDS-PAGE gel

nanoparticles have a good recyclability and stability for extracting of His-tagged recombinant proteins from cell lysate over several separation cycles. In general, a novel magnetic nanomaterial basing on the coordination interaction between Ni^{2+} and the carboxylates coated on the surface of Fe_3O_4 nanoparticles was developed in this work, for fast and efficient His-tagged protein purification, which can be used to improve the separation of His-tagged protein from complex mixture.

Funding This work was supported by the Key Project of Natural Science Research of Universities in Anhui Province (KJ2019A0055), Key Program in the Youth Elite Support Plan in Universities of Anhui Province (gxyqZD2019020 and gxyqZD2020016), and National Natural Science Foundation of China (81872449).

Declarations

Conflict of interest The authors declare no competing interests.

References

1. Zhang YT, Yang YK, Ma WF, Guo J, Lin Y, Wang CC. Uniform magnetic core/shell microspheres functionalized with Ni2+-iminodiacetic acid for one step purification and immobilization of His-tagged enzymes. ACS Appl Mater Inter. 2013;5(7):2626–33. https://doi.org/10.1021/am4006786 .
2. Kadir MA, Kim SJ, Ha EJ, Cho HY, Kim BS, Choi D, et al. Encapsulation of nanoparticles using nitrilotriacetic acid end-functionalized polystyrenes and their application for the separation of proteins. Adv Funct Mater. 2012;22(19):4032–7. https://doi.org/10.1002/adfm.201200849.
3. Cao GX, Gao J, Zhou LY, Huang ZH, He Y, Zhu M, et al. Fabrication of Ni2+-nitrilotriacetic acid functionalized magnetic mesoporous silica nanoflowers for one pot purification and immobilization of His-tagged omega-transaminase. Biochem Eng J. 2017;128:116–25. https://doi.org/10.1016/j.bej.2017.09.019.
4. Woo E-J, Kwon H-S, Lee C-H. Preparation of nano-magnetite impregnated mesocellular foam composite with a Cu ligand for His-tagged enzyme immobilization. Chem Eng J. 2015;274:1–8. https://doi.org/10.1016/j.cej.2015.03.123.
5. Zhang LY, Zhu XJ, Jiao DJ, Sun YL, Sun HW. Efficient purification of His-tagged protein by superparamagnetic Fe3O4/Au-ANTA-Co2+ nanoparticles. Mat Sci Eng C-Mater. 2013;33(4):1989–92. https://doi.org/10.1016/j.msec.2013.01.011 .
6. Liu X, Han HM, Liu HB, Xiao SJ. Enhanced protein loading on a planar Si(111)-H surface with second generation NTA. Surf Sci. 2010;604(15–16):1315–9. https://doi.org/10.1016/j.susc.2010.04.020 .
7. Jose L, Lee C, Hwang A, Park JH, Song JK, Paik HJ. Magnetically steerable Fe3O4@Ni2+-NTA-polystyrene nanoparticles for the immobilization and separation of his(6)-protein. Eur Polym J. 2019;112:524–9. https://doi.org/10.1016/j.eurpolymj.2019.01.024.
8. Masthoff I-C, David F, Wittmann C, Garnweitner G. Functionalization of magnetic nanoparticles with high-binding capacity for affinity separation of therapeutic proteins. J Nanopart Res. 2014;16(1):1–10. https://doi.org/10.1007/s11051-013-2164-6.
9. Tural B, Sopaci SB, Ozkan N, Demir AS, Volkan M. Preparation and characterization of surface modified gamma-Fe2O3 (maghemite)-silica nanocomposites used for the purification of benzaldehyde lyase. J Phys Chem Solids. 2011;72(8):968–73. https://doi.org/10.1016/j.jpcs.2011.05.010.
10. Cao JL, Zhang XH, He XW, Chen LX, Zhang YK. Facile synthesis of a Ni(II)-immobilized core-shell magnetic nanocomposite as an efficient affinity adsorbent for the depletion of abundant proteins from bovine blood. J Mater Chem B. 2013;1(30):3625–32. https://doi.org/10.1039/c3tb20573h.
11. Bilal M, Zhao YP, Rasheed T, Iqbal HMN. Magnetic nanoparticles as versatile carriers for enzymes immobilization: a review. Int J Biol Macromo. 2018;120:2530–44. https://doi.org/10.1016/j.ijbiomac.2018.09.025.
12. Zhou Y, Yan DD, Yuan SF, Chen YW, Fletcher EE, Shi HF, et al. Selective binding, magnetic separation and purification of histidine-tagged protein using biopolymer magnetic core-shell nanoparticles. Protein Expres Purif. 2018;144:5–11. https://doi.org/10.1016/j.pep.2017.11.004.
13. Salimi K, Usta DD, Kocer I, Celik E, Tuncel A. Highly selective magnetic affinity purification of histidine-tagged proteins by Ni2+ carrying monodisperse composite microspheres. RSC Adv. 2017;7(14):8718–26. https://doi.org/10.1039/c6ra27736e.
14. Xu C, Xu K, Gu H, Zhong X, Guo Z, Zheng R, et al. Nitrilotriacetic acid-modified magnetic nanoparticles as a general agent to bind

histidine-tagged proteins. J Am Chem Soc. 2004;126(11):3392–3. https://doi.org/10.1021/ja031776d.
15. Xie HY, Zhen R, Wang B, Feng YJ, Chen P, Hao J. Fe3O4/Au core/shell nanoparticles modified with Ni2+-nitrilotriacetic acid specific to histidine-tagged proteins. J Phys Chem C. 2010;114(11):4825–30. https://doi.org/10.1021/jp910753f.
16. Guo H, Wang W, Zhou F. Fast and highly selective separation of His-tagged proteins by Ni 2+-carrying magnetic core–shell nanoparticles. Appl Phys A-Mater. 2019;125(5):1–10. https://doi.org/10.1007/s00339-019-2631-8.
17. Rashid Z, Naeimi H, Zarnani AH, Mohammadi F, Ghahremanzadeh R. Facile fabrication of nickel immobilized on magnetic nanoparticles as an efficient affinity adsorbent for purification of his-tagged protein. Mat Sci Eng C-Mater. 2017;80:670–6. https://doi.org/10.1016/j.msec.2017.07.014.
18. Wu SL, Chen JR, Ma L, Zhang K, Wang XX, Wei YP, et al. Design of carbonic anhydrase with improved thermostability for CO2 capture via molecular simulations. J CO2 Util. 2020;38:141–7. https://doi.org/10.1016/j.jcou.2020.01.017.
19. Yang X, Zhang M, Zheng J, Li W, Gan W, Xu J, et al. Ni nanoparticles decorated onto graphene oxide with SiO2 as interlayer for high performance on histidine-rich protein separation. Appl Surf Sci. 2018;439:128–38. https://doi.org/10.1016/j.apsusc.2017.12.227.
20. Wang Y, Wang G, Xiao Y, Yang Y, Tang R. Yolk–shell nanostructured Fe3O4@ NiSiO3 for selective affinity and magnetic separation of His-tagged proteins. ACS Appl Mater Inter. 2014;6(21):19092–9. https://doi.org/10.1021/am505041a.
21. Ding C, Ma X, Yao X, Jia L. Facile synthesis of copper (II)-decorated magnetic particles for selective removal of hemoglobin from blood samples. J Chromatogr A. 2015;1424:18–26. https://doi.org/10.1016/j.chroma.2015.11.004.
22. Zhang CC, Kuai Y, Cheng HM, Liu X, Ma L. Covalent bonding of grafted polymer brushes of poly(poly(ethylene glycol) monomethacrylate) on surface of silicon quantum dots and the activation of the end hydroxyls. Ara J Chem. 2019;12(8):5260–7. https://doi.org/10.1016/j.arabjc.2016.12.022.
23. Lu KP, Zhou XZ. The prolyl isomerase PIN1: a pivotal new twist in phosphorylation signalling and disease. Nat Rev Mol Cell Bio. 2007;8(11):904–16. https://doi.org/10.1038/nrm2261.
24. Chang MM, Qin Q, Wang BH, Xia T, lv WJ, Sun XS, et al. Carboxymethylated polyethylenimine modified magnetic nanoparticles specifically for purification of His-tagged protein. J Sep Sci. 2019;42(3):744–53. https://doi.org/10.1002/jssc.201800969.
25. Rashid Z, Ghahremanzadeh R, Nejadmoghaddam MR, Nazari M, Shokri MR, Naeimi H, et al. Nickel-Salen supported paramagnetic nanoparticles for 6-His-target recombinant protein affinity purification. J Chromatogr A. 2017;1490:47–53. https://doi.org/10.1016/j.chroma.2017.02.014.
26. Shirzadi Z, Baharvand H, Nezhati MN, Sajedi RH. Synthesis of nonlinear polymer brushes on magnetic nanoparticles as an affinity adsorbent for His-tagged xylanase purification. Colloid Polym Sci. 2020;298(11):1597–607. https://doi.org/10.1007/s00396-020-04749-7.
27. Zou X, Li K, Zhao Y, Zhang Y, Li B, Song C. Ferroferric oxide/l-cysteine magnetic nanospheres for capturing histidine-tagged proteins. J Mater Chem B. 2013;1(38):5108–13. https://doi.org/10.1039/c3tb20726a.
28. Rashid Z, Naeimi H, Zarnani AH, Nazari M, Nejadmoghaddam MR, Ghahremanzadeh R. Fast and highly efficient purification of 6×histidine-tagged recombinant proteins by Ni-decorated MnFe2O4@SiO2@NH2@(2)AB as novel and efficient affinity adsorbent magnetic nanoparticles. RSC Adv. 2016;6(43):36840–8. https://doi.org/10.1039/c5ra25949e.